

## Shallow Geophysical Techniques for Groundwater Aquifer Exploration, Ain Alsokhona Area, West Gulf of Suez, Egypt

Othman A. A. A.<sup>1</sup>, Abd El Hafez Th. H.<sup>1</sup>, Youssef M.A.S.<sup>2</sup> and Sabra M. E. M.<sup>3</sup>

<sup>1</sup>Geology Department, Faculty of Science, Al-Azhar University, Cairo, Egypt.

<sup>2</sup>Nuclear Materials Authority, Exploration Division, Po. Box 530, Maadi, Cairo, Egypt.

<sup>3</sup>Egyptian Mineral Resources Authority, Po. Box 11517, Abbassiya, Cairo, Egypt.

[Shokryam@yahoo.com](mailto:Shokryam@yahoo.com)

**Abstract:** Eight seismic refraction profiles, five Vertical Electrical Soundings (VES) and four geophysical well logging tools were acquired along the western side of Gulf of Suez, Egypt, in order to study the aquifer's geometry, groundwater level and locate promising sites for future drilling. The well logging measurements included: natural gamma-ray (GR), self potential (SP), electric resistivity (16", 64"), density and neutron. The seismic primary wave velocity distribution indicated that, there are three different zones ranging between (500 – 625 m/s), (1300 – 1600 m/s) and (2400 – 3000 m/s). The obtained results showed that, the first low velocity range may indicate an unsaturated zone, which is directly affected by surface water, that appears along the studied area. The second and third velocity ranges may show water level at saturated zone and the lithologic interfaces. The estimated thickness of the unsaturated zone varies between 1 m and 3.5 m. The thickness of the top saturated zone ranges between 9.5 m and 26 m. This represents the gradual increase of seismic velocity layers with depth. This increase may be due to the dense formations, which change vertically from alluvial at the surface to compacted sediments and then to sandstone at depth. The true resistivity of the aquifer shows two zones; the first zone is a surficial resistive layer of dry alluvium, unconsolidated with consolidated Wadi sediments, which have average resistivity of more than 440  $\Omega \cdot m$ , then lower resistivities reaching to 21  $\Omega \cdot m$  in the second zone, which constitutes the main aquifer in the third and fourth geoelectric layers. The geophysical well logging tools confirm the water depths obtained from the seismic refraction analysis and vertical electric soundings. The water table levels are start below 17, 40, 15 and 45 m at wells No 1, 2, 3 and 4, respectively. In addition, they give more detailed explanation to the subsurface lithologies and their physical properties through varying lithologies with depth, such as porosity, clean or radioactivity, density and electrical resistivity. The integration of these results confirms the existence of a groundwater aquifer within this interval. The combination between the three executed geophysical methods indicated that, the subsurface lithology of the area is composed of three layers. The first top layer is formed from unconsolidated and consolidated Wadi sediments (unsaturated zone). The second saturated zone is a fractured rock; it is composed mainly of saturated sandstone and considered a promising layer for groundwater accumulation. The surface level of groundwater increases to the west, and decreases to the east of the study area. The obtained results show that, any future drilling for groundwater, a number of VES positions may be considered as potential locations, especially at VES 3.

[Othman A. A. A., Abd El Hafez Th. H., Youssef M.A.S. and Sabra M. E. M. **Shallow Geophysical Techniques for Groundwater Aquifer Exploration, Ain Alsokhona Area, West Gulf of Suez, Egypt.** *Researcher* 2013;5(6):30-41]. (ISSN: 1553-9865). <http://www.sciencepub.net/researcher>. 6

**Keywords:** VES, Seismic Refraction, Neutron Log and Groundwater.

### 1. Introduction

Groundwater resources play a vital role in the spreading of urbanization and encouragement of investments in Ain Alsokhona area. Consequently, groundwater resources of Ain Alsokhona area were intensively investigated by many workers (Eldiasty et al., 1981; Abuelata and Hassan, 1990; Abdellateif et al., 1997; Elbeheiry et al., 2004) and many others).

The seismic refraction method and vertical electrical sounding (VES) are important geophysical methods to attain success in this aim. They were adopted to investigate the probability of fresh groundwater occurrence in the study area. The objective of the seismic and geoelectric measurements is to confirm or not this assumption, that the

groundwater accumulation can primarily be revealed by seismic refraction technique, especially in the gravely-sands or silty clay areas, in which the groundwater level can be determined as a boundary of acoustic impedance (Galfi and Palos, 1970). Shallow seismic survey can be very useful when integrated with vertical electrical sounding (VES) and confirmed by well logging measurements, in order to investigate changes in the groundwater level and possibly locate the fresh groundwater aquifer and other promising sites for future drilling in the study area.

### Location and Geologic Setting

Ain Alsokhona area is a region in the Suez Governorate and is located on the western side of

Gulf of Suez, Egypt (Fig.1). Geomorphologically, Ain AlSokhona area could be divided into four main units (Conoco; 1987; Salem, 1988 and Said, 1990), as follows: 1) Coastal plain unit: It is represented by a low land that occur between Gulf of Suez to the east and a hilly and mountain terrain further west. It is mainly covered by Quaternary clastic, extensive thick gravely and sandy sediments forming a gently seaward sloping plain. 2) A high land unit: It is represented by Gabal Ataqa, Northern Galala, and the plateaus. Gabal Ataqa is a bold mountain block forming high vertical scarps (their northern and eastern sides) reaching highest point of about 900 m above sea level, and the Northern Galala which represents a great massive block situated in the northern part of the Gulf of Suez. 3) A low lying hill unit: It is mainly covered by Upper Eocene, Oligocene and Miocene rocks. 4) The drainage pattern: It is defined by four major drainage basins in Ain Alsokhona area. These basins from north to south are: Wadi Hagoul and then Wadi located to the south of Wadi Hagoul, Wadi Akheider bada and Wadi Ghoweibba.

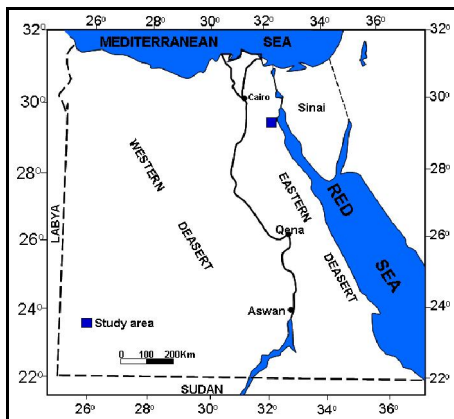


**Fig. 1: Location map of Ain El-Sokhna area, Egypt.**

Regional lithologic units and structures were observed and investigated thoroughly in the field as shown on Fig. (2). Abu-Elenain and Ismail, (1995) divided the Eocene rocks into; Middle Eocene (Mokattam Formation) and Upper Eocene (Maadi Formation). The Oligocene rocks unconformably overlie the Upper Eocene clastics. Oligocene rocks appear in two different types: volcanic rocks (basaltic sheets and doleritic intrusions), which overlie the Upper Eocene clastic rocks, and sedimentary rocks (sandstone, quartzite and flint gravel), which are overlain by Lower Miocene rocks. Miocene rocks consist of, from top to bottom: Hagoul Formation (Upper Miocene) and Sadat Formation (Lower Miocene). The Pliocene sediments consist mainly of a

series of gravels and flint pebbles in a sandy matrix, meanwhile in some other parts, these gravels consist of a mixture of flint and limestone pebbles as well as in a sandy matrix (Salem, 1988). Quaternary sediments are represented by Holocene and Pleistocene, which are made up of gravels, cobbles, boulders and sands in the form of Quaternary terraces and alluvium.

Youssef and Abdel Rahman (1978) considered the study area as a huge graben, in which numerous gently tilted fault blocks protrude above the general surface. Salem (1988) analyzed the structural features of the study area to identify its deformational style that affected the area and the probable stress directions. He also pointed out the relation between the style of deformation and two provinces (Gulf of Suez to the east and the Cairo-Suez district to the north). He mentioned that the majority of the faults are normal and few of these are diagonal-slip, with major dip-slip and minor strike-slip components.

## 2. Methodology and Data Acquisition Shallow Seismic Refraction Survey

Seismic refraction method uses the seismic energy that returns to the surface after traveling through the ground along refracted ray paths. The first arrivals of the seismic energy to a detector offset from a seismic source always represent either a direct ray or a refracted ray (Reynolds, 1997). The compressional wave velocity increases the confining pressure. The sandstone and shale velocities show a systematic increase with depth of burial and with age, due to the effects of progressive compaction and cementation. Shallow seismic survey was carried out using a seismograph Model-1125E McSEIS-SX, 12, highly sensitive vertical geophones and a sledge Hammer energy source of 10 kg. Two off-end spreads (forward and reverse) were designed for this survey, according to the available geological information and the main aim of the study.

Eight seismic refraction profiles were acquired in the study area. The profile extensions were 120 meters in length and trend in the NW-SE direction. Forward, reverse, split and offset seismic shootings were carried out with a geophone interval of 10 meters. The locations of these profiles in the study area are shown on a map (Fig.3).

The seismogram is the main result of field work. It represents the analog recording of the received signals. The recorded seismic traces reflect the responses of the subsurface interfaces. Figure (5A) shows an example of the seismogram of a split shot of the first spread. The most important first arrivals are the direct and refracted waves, were received by

the geophones. Some of the recorded traces were noisy or bad traces, even after applying filtering techniques during processing stage, which was carried out to enhance the signal/noise ratio. These bad or high noisy traces were discarded or deleted from some of the shot records.

The picked first-arrival times were inverted into corresponding depth-velocity sections (geoseismic cross sections) using Winsism 9 software (2009), based on the Generalized Reciprocal Method (GRM).

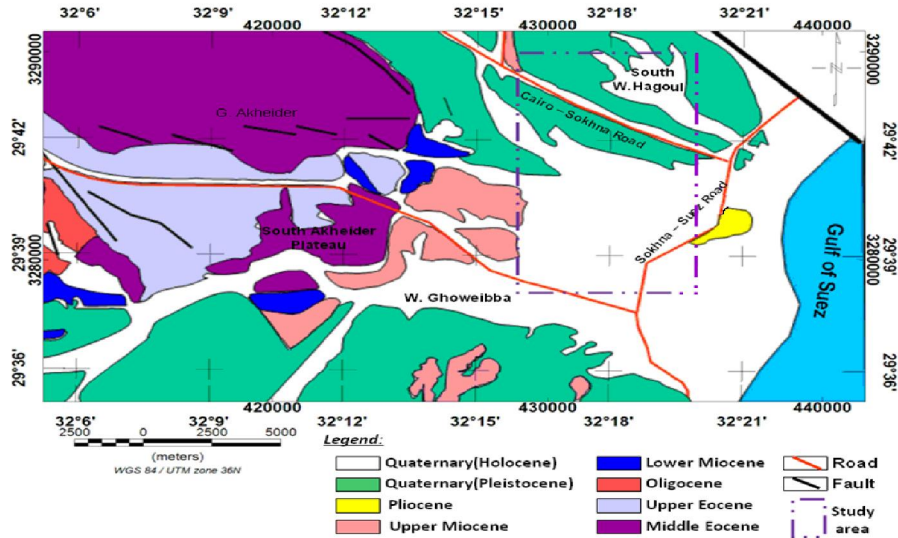


Fig. 2: Regional geologic map of the study area (after, Conoco 1987).

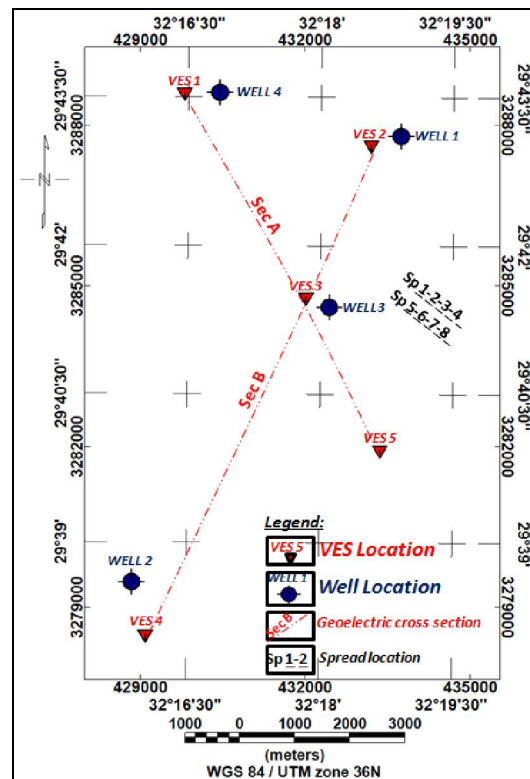
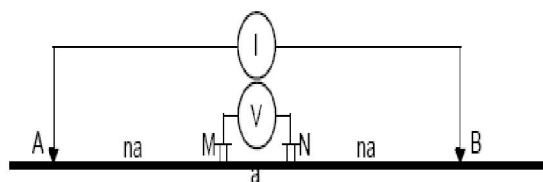


Fig. 3: Location map of seismic refraction spreads, VESes, geoelectric cross section and Drilled wells of the study area.

**Vertical Electrical Sounding (VES)**

Resistivity surveys measure the composite electrical resistivity of the subsurface. Direct current is induced into the ground between two current electrodes A and B and the potential difference is measured between two potential electrodes M and N (Fig. 4). A resistance value is obtained by dividing the measured voltage (V) by the induced current (I). The apparent resistivity is calculated from the resistance value and geometrical factor, that accounts for the electrode spacing configuration.

In the present study, the electrical resistivity measurements were carried out using Schlumberger array configurations (Zohdy, 1974). This array remained as one of the best arrays for depth sounding among the different array configurations. The main application of this array is to explore the groundwater aquifer occurrences. In this method, the center point of the electrode array remains fixed, but the spacings between electrodes are increased progressively to obtain more information about the deeper sections of the subsurface (Fig. 4).



**Fig. 4: Sketch diagram showing the Schlumberger electrode arrays.**

The Vertical Electrical Sounding (VES) survey was conducted at 5 sites distributed in the study area (Table 1 and Fig. 3). The VES specifications were selected as seven measurements per decade to obtain excellent data continuity, while half current electrode spacing (AB/2) started from one meter to 500 meter. The equipment used in the present study is ELREC-T, IRIS Instruments, France, with a microprocessor, digital display and RS-232C interface for the PC data dump. From the field data, the apparent resistivities ( $\rho_a$ ) were plotted versus AB/2 on a log-log paper. The advantages of log-log plot is that it emphasizes the near-surface resistivity variations and suppresses the variations at greater depths. This is important, because the interpretation of the results depends largely on small variations in the resistivities occurring at shallow depths.

The VESes field data were interpreted through successive interpretation steps. Feeding the field data to a PC represents the first step, in order to get the n-layer model. The interpretation of the VESes was obtained through using an automatic interpretation

multi-layer computer program (Zohdy and Bisdorf, 1989). Based on these interpretations, the parameters of  $\rho$  (resistivity), d (depth) and h (thickness) of a geoelectric model, thought to be closer to reality, were estimated.

**Table (1): 5 VES's locations in the study area.**

VES No.	Coordinates			
	Lat / long		UTM	
1	29° 43' 32" N	32° 16' 27" E	429804 E	3288618 N
2	29° 43' 01" N	32° 18' 33" E	433198 E	3287633 N
3	29° 41' 26" N	32° 17' 56" E	432175 E	3284726 N
4	29° 38' 04" N	32° 16' 02" E	429080 E	3278507 N
5	29° 39' 56" N	32° 18' 40" E	433353 E	3281945 N

**Geophysical Well Logging**

Four wells were drilled by the Egyptian Geological Survey and Mining Authority (EGSMA) in the study area. They are located near the seismic refraction survey and VES's area (Fig. 3). They showed the different types of layers within the area under examination. Well logging measurements included in Natural Gamma (GR) for measuring total radiation, Self Potential (SP) for delineating line base mud and lithologic contact, Electric Resistivity (16" & 64"), for measuring the resistivities of the flushed zone, and the true formation respectively, Density log for displaying rock density and Neutron log, that illustrates the rock porosity.

**4. Discussion and Interpretation**

The results obtained from shot records (Table 2) and their interpretations indicate that the P-wave Velocities can be determined as: 1) Unconsolidated Wadi sediments at the top having P-wave velocities range of ( $V_{p1}=500 - 625$  m/s), in which the thickness of this layer varies between 1.0 and 3.5 m. 2) The second layer velocities range of ( $V_{p2}=1300-1600$  m/s), which corresponds to consolidated Wadi sediments and show the surface of water at this layer. The thickness of this layer varies between 9.5 and 26 m; and 3) The third layer is characterized by high average seismic velocity ranges of  $V_{p3}=2400-3000$  m/s, that corresponds to fractured sandstone layer.

These velocity ranges may represent the bed interfaces. It is noticed that, the refracting velocity at the water level is the lowest when the water level is at the shallowest depth. When the water level drops closer to the top of the saturated zone, refracting velocities are observed to increase. However, as the



water level drops close to the saturated zone, it may become undetectable. One example of seismogram of split shot and the time-distance curve of the first spread in the study area is shown on Fig. (5 A and B) and the eight geoseismic cross sections in the study area which reflect three main seismic layers (Fig. 6A to 6H).

The resultant multi-layer model for VES (1), using Ato program (Zohdy and Bisdorf, 1989), is shown as an example is shown in (Fig. 7A). It represents the initial model used for feeding the Resist layering program (Velpen, 1988) and constructing the subsurface true resistivity contour sections. The five layering models of Resist program (Figs. 7B to 7F) were used to reduce the layers to 4, in order to build up a geoelectric model. The results of these VES's are resistivity, thickness and depth, as summarized in Table (3).

According to the behaviour of field curves and

the number of subsurface geoelectric layers for each sounding, VES results indicate that the true resistivities of the aquifer reflect first a surficial resistive layer of dry alluvium with a resistivity ranging between 440 and 3600 Ω.m, then a lower resistivity, which reaches 440 Ω.m at VES 5, followed by the highest resistivity, which attains 3655 Ω.m at VES 2. The second geoelectric layer is characterized by gravel, sand and loose sand, which possesses an average resistivity of 200 Ω.m and an average depth of 2.5 m. The third and fourth geoelectric layers represent the best aquifer, which have low resistivity values of less than 100 Ω.m. According to Bernard (2003), in order to identify the presence of groundwater from resistivity measurements, one can look to the absolute value of the ground resistivity: for a practical range of fresh water resistivity of 10 to 100 Ohm.m.

**Table 2: Velocity parameters of the geoseismic layers.**

Spread No.(Sp)	(GI)&(SL) and (DS)	Character of layer	Geoseismic Layers ( GSL)		
			Layer (1)	Layer (2)	Layer (3)
Sp 1 (Fig.6A)	10&120m (NW-SE)	Velocity (m/s)	550 - 625	1350 - 1550	2300 - 2600
		Thickness (m)	1.3 - 2.5	17 - 19	-----
		Top of layer (m)	12 - 16	11 - 13.5	(-4.5) - (-7)
Sp 2 (Fig.6B)	10&120m (NW-SE)	Velocity(m/s)	550 - 600	1400 - 1600	2600 - 3000
		Thickness(m)	1 - 2.5	15.5 - 18	-----
		Top of layer (m)	11 - 17.5	10 - 13	(-3) - (-8)
Sp 3 (Fig.6C)	10&120m (NW-SE)	Velocity(m/s)	500 - 600	1400 - 1550	2200 - 2600
		Thickness(m)	1 - 2.5	18 - 26	-----
		Top of layer (m)	15.5 - 19	15 - 18	(-1) - (-8)
Sp 4 (Fig.6D)	10&120m (NW-SE)	Velocity(m/s)	550 - 600	1400 - 1600	2200 - 2600
		Thickness(m)	1 - 2	20.5 - 24.5	-----
		Top of layer (m)	15 - 18	14 - 17	(-4) - (-8)
Sp 5 (Fig.6E)	10&120m (NW-SE)	Velocity(m/s)	500 - 600	1300 - 1500	2600 - 2900
		Thickness(m)	2.5 - 3.5	9.5 - 12.5	-----
		Top of layer (m)	17.5 - 20	14 - 16	2.5 - 6
Sp 6 (Fig.6F)	10&120m (NW-SE)	Velocity(m/s)	550-600	1300 - 1500	2400 - 2600
		Thickness(m)	1 - 1.5	17 - 23	-----
		Top of layer (m)	14 - 18	12.5 - 15	2 - (-8)
Sp 7 (Fig.6G)	10&120m (NW-SE)	Velocity(m/s)	500 - 600	1400 - 1600	2200 - 2600
		Thickness(m)	1.5 - 2.4	17 - 26	-----
		Top of layer (m)	19 - 23	18 - 21	2 - (-5)
Sp 8 (Fig.6H)	10&120m (NW-SE)	Velocity(m/s)	500 - 600	1400 - 1500	2800 - 3000
		Thickness(m)	1.2 - 2.5	12 - 19	-----
		Top of layer (m)	19 - 22	18.5 - 21	1.5 - 5
<b>Integrated geology &amp; GSL</b>			<b>UCWD</b>	<b>CWD</b>	<b>S.S</b>

Explanation:

Sp is the spread,  
GI is the geophone interval,  
SL is the spread length and  
DS is the direction of spread.

Interpreted geology:

UCWD is the Unconsolidated Wadi Deposits.  
CWD is the Consolidated Wadi Deposits.  
S.S is the Sandstone layer.

The measured apparent resistivities were then presented in a contoured pseudo section, which

reflect qualitatively the spatial variation in resistivity in the vertical cross-section (Griffiths and Turnbull,

1985). Therefore, the interpretation of VES data was carried out using the subsurface true resistivity contour sections (Figs. 8A and 9A) and the geoelectric cross sections (Figs. 8B and 9B), as well as the individual soundings. Careful examination of the subsurface sections can provide useful

information about the subsurface lithology, structure and groundwater occurrence. It can also give additional information about the lateral discontinuities in subsurface lithology (Sadek et al., 1989).

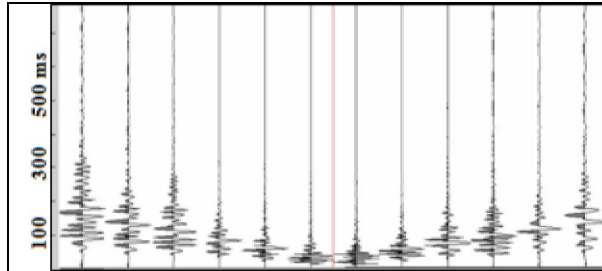


Fig. 5A: Seismogram of split shot of the first spread.

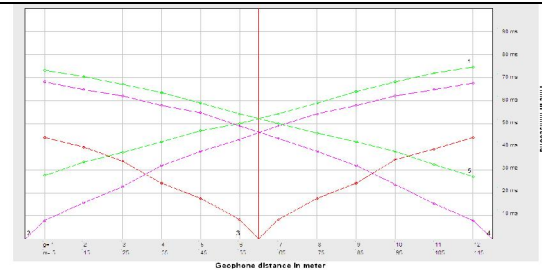


Fig. 5B: Time-Distance curve of spread (1) in the spot area.

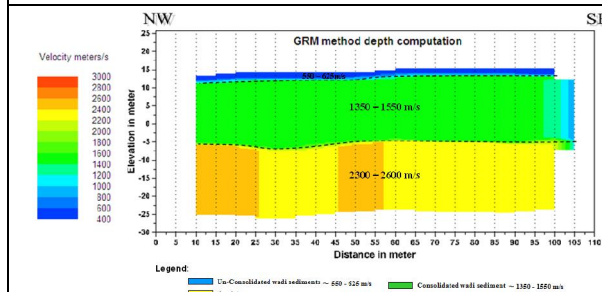


Fig. 6A: Geoseismic cross section of spread (1) by GRM.

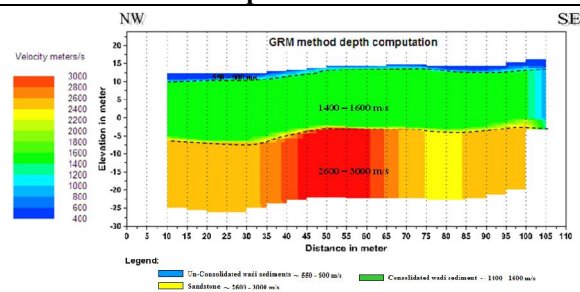


Fig. 6B: Geoseismic cross section of spread (2) by GRM.

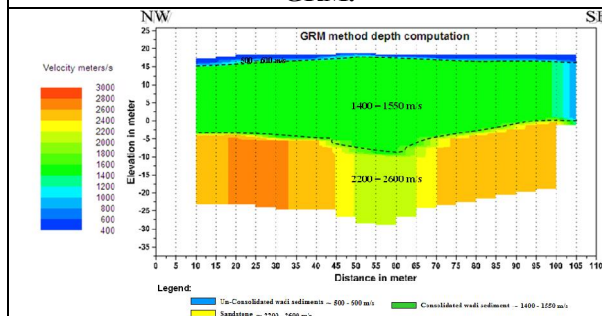


Fig. 6C: Geoseismic cross section of spread (3) by GRM.

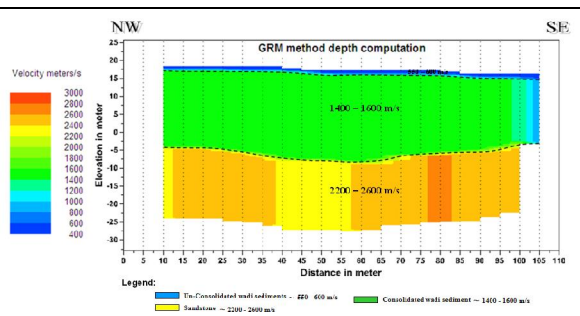


Fig. 6D: Geoseismic cross section of spread (4) by GRM.

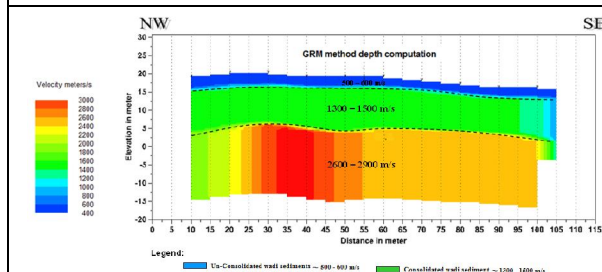


Fig. 6E: Geoseismic cross section of spread (5) by GRM.

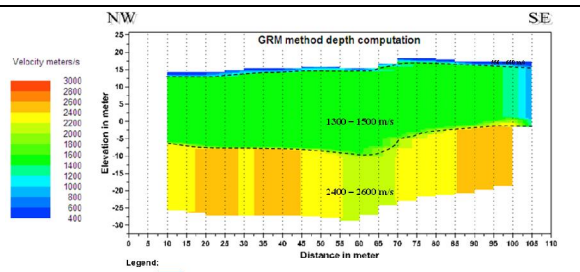
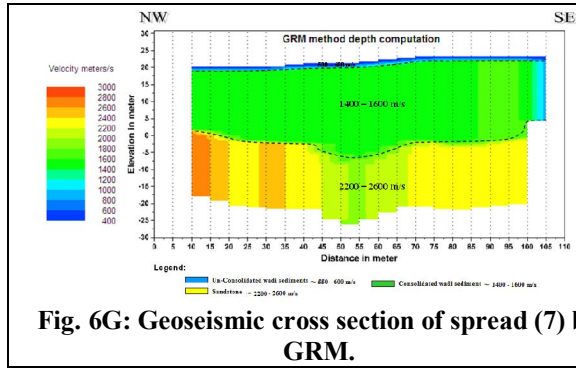
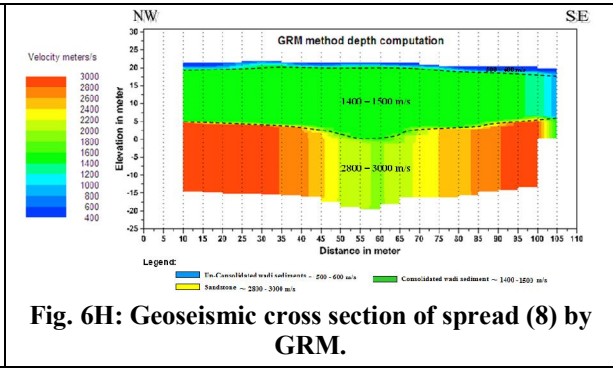


Fig. 6F: Geoseismic cross section of spread (6) by GRM.



**Fig. 6G: Geoseismic cross section of spread (7) by GRM.**



**Fig. 6H: Geoseismic cross section of spread (8) by GRM.**

**Table 3: Resistivity parameters of geoelectric layers from Resist layering program (Velpen, 1988).**

VES No.	Parameters	Geoelectric Layers			
		1	2	3	4
VES 1	$\rho$ (Ohm.m)	839.6	15.8	6	22.1
	$h$ (m)	1	6.7	43.7	-
	$d$ (m)		1	7.2	51
VES 2	$\rho$ (Ohm.m)	3655	700	100	21
	$h$ (m)	3	9	54.5	-
	$d$ (m)		3	12	66
VES 3	$\rho$ (Ohm.m)	1429	60.4	15.8	9.6
	$h$ (m)	3.8	19.9	85.8	-
	$d$ (m)		3.8	23.7	110
VES 4	$\rho$ (Ohm.m)	2036	244	26.3	70.8
	$h$ (m)	2	9.5	93.8	-
	$d$ (m)		2	11.5	105
VES 5	$\rho$ (Ohm.m)	444.2	118.7	18	7.8
	$h$ (m)	1.6	24.9	49.5	-
	$d$ (m)		1.6	26.4	75.9

Explanation:  $\rho$  is the true resistivity value,  $h$  is the thickness of layer and  $d$  is the depth of layer.

Two geoelectric cross sections were constructed, which illustrate the distribution of the different geoelectric layers in the study area (Fig. 3). A-A<sup>\</sup> and B-B<sup>\</sup> sections will be illustrated hereafter. It is worth mentioning that, the first geoelectric layer (unconsolidated Wadi sediments) is very thin and highly resistive layer. Its thinning character causes it to be unrecognizable in the 2D geoelectric cross section. So, to avoid misinterpretation, the first layer (unconsolidated sediments) and the second layer (consolidated sediments) were joined together, representing Wadi sediments in the integration of VES data with both the seismic and well logging data.

The study area could be subdivided into two zones, based on the difference in their resistivities; the northern, central and southern parts. The first geoelectric cross section, A-A<sup>\</sup> (Fig. 8) passes through VESes 1, 3 and 5 from the northwest to the southeast. The first zone of soundings 1, 3 and 5 reflects the presence of four geoelectric layers. The first and second layers (Wadi sediments) attain average

thicknesses of about 8 m and 28 m respectively. The third and fourth layers represent the fractured porous rock at an average depth of 21 m.

The second zone is located deeper in VESes 3 and 5 than VES 1. This zone may represent the beginning of the aquifer, because its resistivity ranges between 8 and 22 Ohm.m. So, it represents the promising layer for groundwater accumulation. Structurally, the two normal faults (F<sub>1</sub> and F<sub>2</sub> (Fig. 8 and 9)) cause of the down-faulting of the block at the central part. It represents a graben structure. The two bounding faults of the graben block are trending in the SE and NW directions.

Meanwhile, the second geoelectric cross section, B-B<sup>\</sup> (Fig. 9) passes through VESes 2, 3 and 4 from the northeast to the southwest of the study area. The layering models of the soundings 2, 3 and 4 reflect the presence of four geoelectric layers. The combination of the first and second layers show a thicknesses of 14 m, 28 m and 13 m respectively, while the third and fourth layers represent the rock containing underground water.

The groundwater aquifer in the study area is mainly composed of two different layers with different characteristic features, taking into consideration the groundwater movement and the

different factors affecting this movement, such as the dipping of layers and their porosities. Structurally, two normal faults (F<sub>3</sub> and F<sub>4</sub>) cause the down-faulting the block in the SW direction.

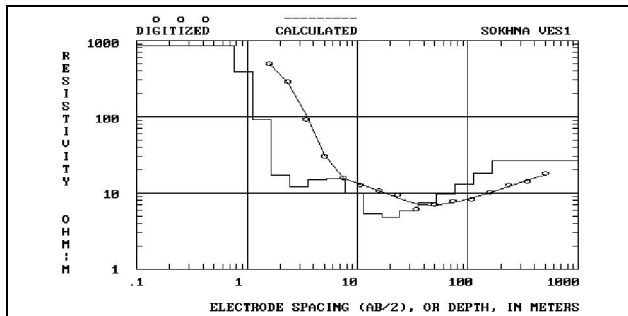


**Fig. 7A: Geoelectric multi-layer modeling of VES (1) using Ato program (Zohdy, 1989) as an example**

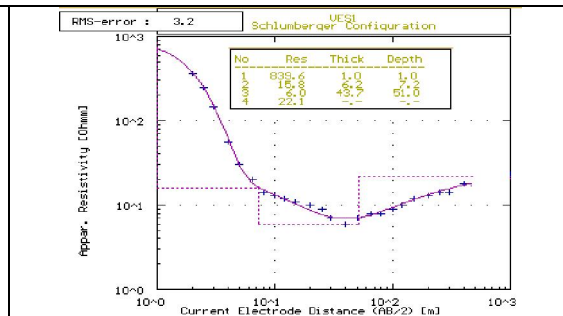


**Fig. 7B: Geoelectric layer modeling of VES (1) using Resist (Velpen, 1988).**

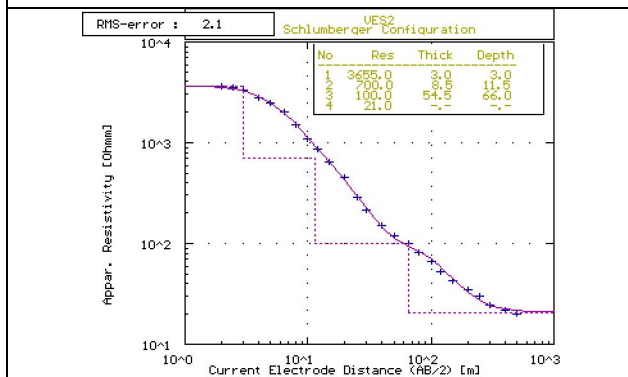


**Fig. 7C: Geoelectric layer modeling of VES (2) using Resist (Velpen, 1988).**

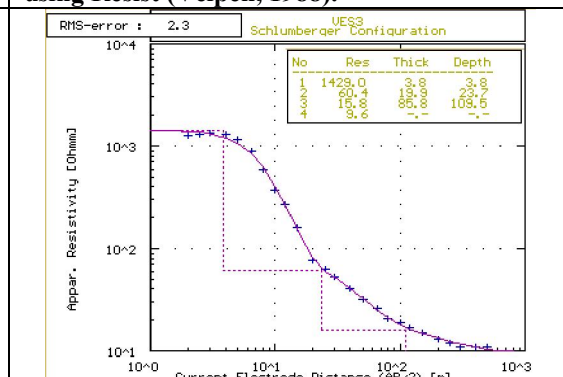


**Fig. 7D: Geoelectric layer modeling of VES (3) using Resist (Velpen, 1988).**

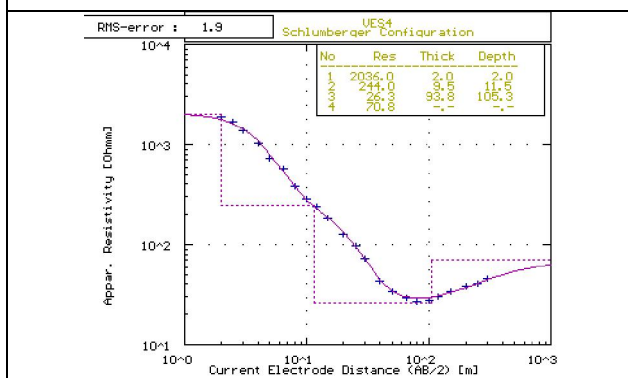


**Fig. 7E: Geoelectric layer modeling of VES (4) using Resist (Velpen, 1988).**

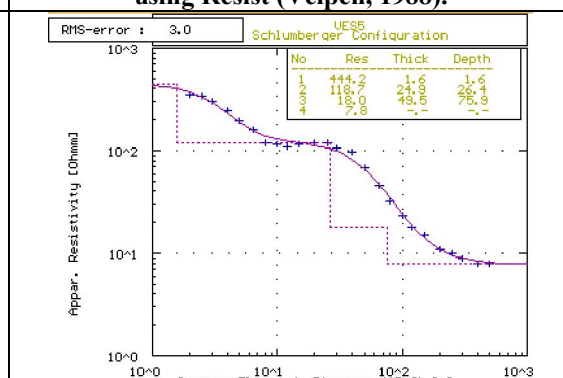


**Fig. 7F: Geoelectric layer modeling of VES (5) using Resist (Velpen, 1988).**



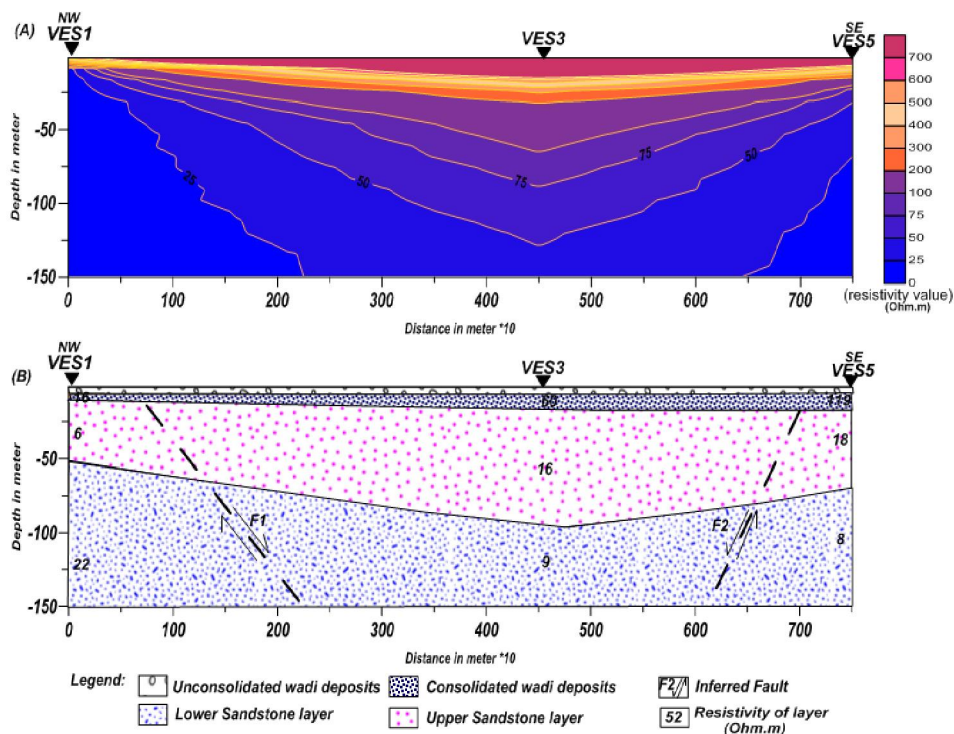


Fig. 8: (A) Subsurface true resistivity contour section A-A' and (B) 2D geoelectric cross section A-A' passing through VES's 1, 3 and 5.

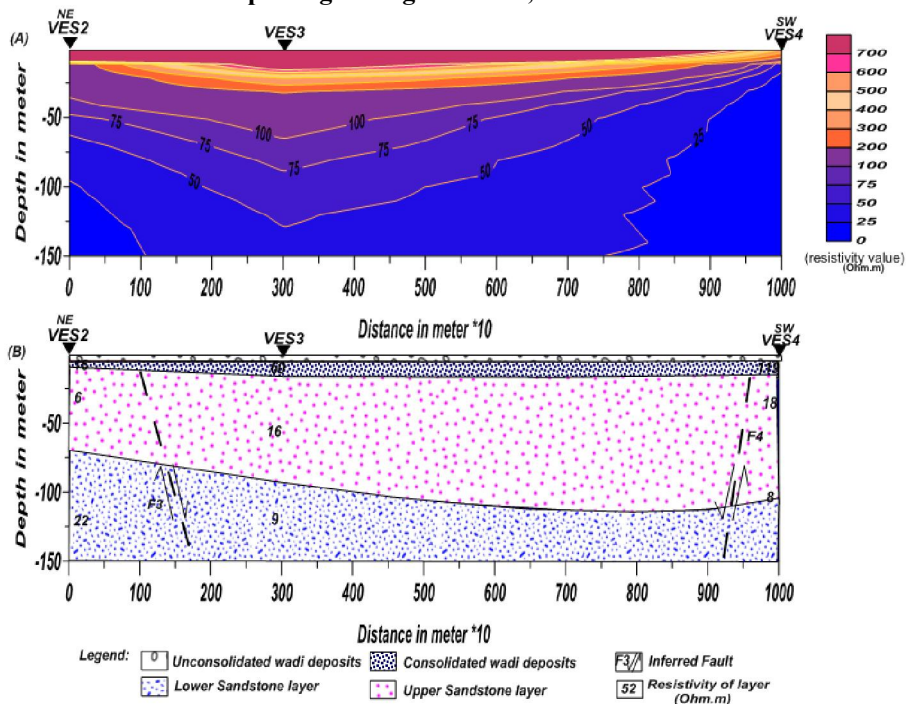
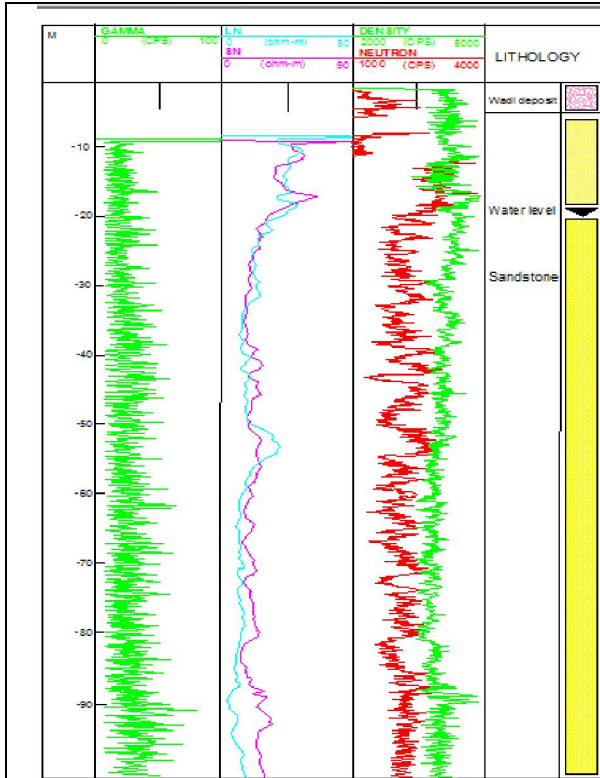


Fig. 9: (A) Subsurface true resistivity contour section B-B' and (B) 2D geoelectric cross section B-B' passing through VES's 2, 3 and 4.

Well logging measurements included: Natural Gamma ray (GR), Self Potential (SP), Electric Resistivity (16", 64"), as well as Density and Neutron logs. Figures (10A to 10D) show that well logging

data of these drilled wells through out the examined area. These four figures indicate that, surface of groundwater is thought to be at 100 m depth at least.



**Fig.10A: Well logging data of the upper part of well No.1.**

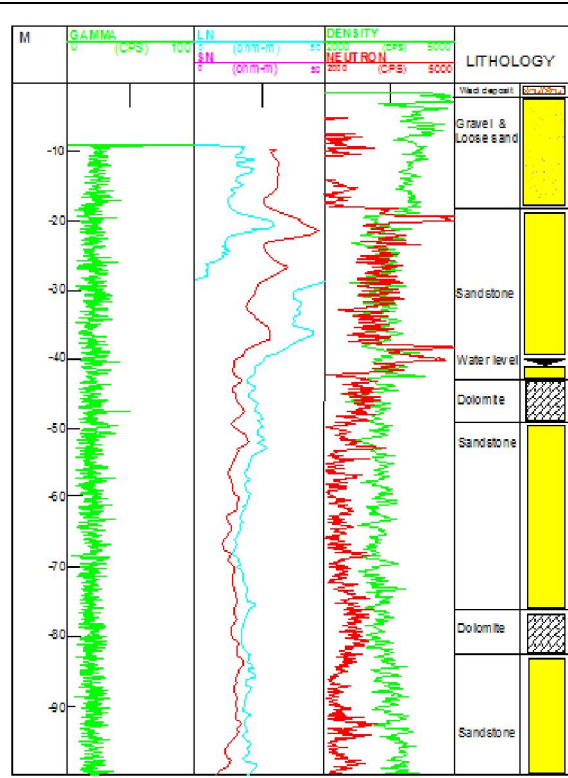


**Fig.10B: Well logging data of the upper part of well No.2.**

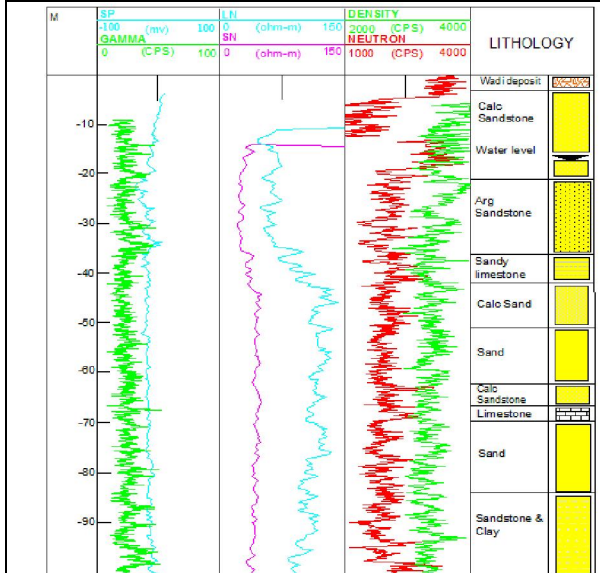


**Fig.10C: Well logging data of the upper part of well No.3.**

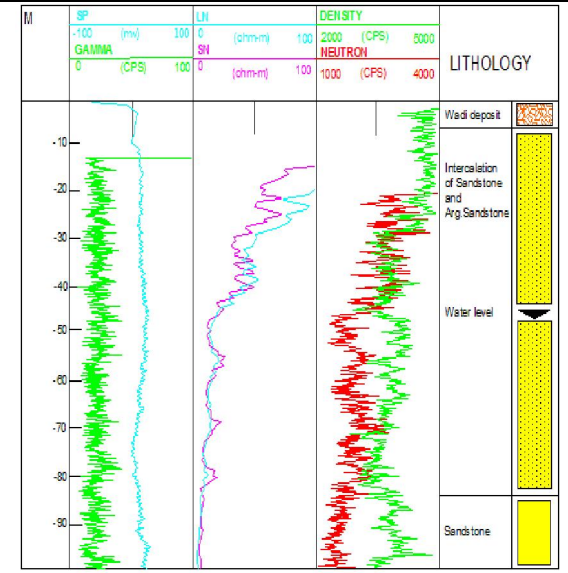


**Fig.10D: Well logging data of the upper part of well No.4.**

Well No. 1 (Fig. 10 A) is composed mainly of a sandstone section which exceeds 100 m, as well as some Wadi sediments of less than 10 m at the top. The low intensity gamma-ray log indicates a clean formation that is of very low radioactivity. The electrical resistivity logs confirm the occurrence of a

good aquifer, where the measurements ranges about 15 Ohm.m, and the water level started below 17 m, as was indicated and confirmed from both neutron and resistivity curves.

The wire-line logging of the second well yielded at direct indication for both lithology and fluid

content, in which the well penetrated Wadi sediments, gravel, loose sands and a long sandstone section, interbedded, sometimes with dolomites. The target aquifer in the well area was met at 40 m, which was confirmed with resistivity logs (around 20 Ohm.m) and neutron log (40 m depth). The aquifer represents a clean fresh water-bearing formation, which was confirmed by natural gamma logging (Fig.10 B). the water may prove to be potable (drinkable).

Lithologically, the third well (Fig.10 C) is composed of a sandstone section below Wadi weathered sediments. This sandstone cement is calcareous, becoming argillaceous in parts and interbedded with limestone in others. The electric logs suite can be interpreted from the long normal resistivity (LN) curve which is relatively lower than the other wells, giving rise to 120 Ohm.m. Meanwhile, the short normal resistivity (SN) reaches more than 40 Ohm.m. These values indicate perfect fresh-water aquifer that below 15 m depth. Neutron and resistivity curves confirmed this water table depth. The gamma-ray log shows a clean formation at different depths in this well.

The fourth well, penetrates Wadi deposits, along a sandstone section becoming argillaceous in some intervals. At a depth of 45 m, the water table is encountered as indicated from both neutron and resistivity curves. The formation shows very low radioactivity, which is considered clean as far as radioactivity is concerned. The resistivity logs indicate a saline water sandstone reservoir, in which the measurements are less than 20 Ohm.m. The formations show very low radioactivity, which is considered clean formations from radioactive materials.

The integrated seismic refraction profiles, VESes and well logging techniques showed that the aquifer is a Quaternary alluvial sediments aquifer, which consists mainly of gravels, sands and clays that is underlain by sandstone. The northern part of the study area includes VESes Nos 1 and 2, as well as wells Nos 1 and 4. The study area shows good agreement in the average level of water table of 17 m depth in VES 2 and in well No 1. Nevertheless, in case of VES No 1 and well No 4, the water table is noticed at an average depth of 45 m for the fourth geoelectric layer and the fourth well. The central part of the study area included VESes Nos 3 and 5, well No. 3 and eight seismic spreads. The water table was noticed at 11 m under VES 3, from 7 to 14 m in the seismic spreads, and 15 m in well No. 3. The southern part of the study area is represented by well No. 2 and VES No. 4. It was found that, the static water table was detected at 27 m depth in VES No. 2 and 40 m in the drillhole 2. The total saturated thickness of the unconfined aquifer reaches more than 55 m.

## Summary and Conclusions

A geophysical survey was planned and executed, which aims to integrate seismic refraction spreads, resistivity soundings and well logging data to delineate the subsurface geologic and hydrogeologic conditions of the groundwater status Ain AlSokhona area, West Gulf of Suez, Northern Eastern desert, Egypt. Inversion of seismic refraction data revealed that the second layer has P-wave velocity of about 1300-1600 m/s and may be considered a good indicator to underground water in the study area.

The application of geoelectric study showed that the sandstones in the area are highly fractured and filled with water at depths of 11 to 26 m. Resistivity sounding inversion data indicated that the aquifer possesses a resistivity range of 6-100 Ohm.m. The study area is affected by nearly linear structural elements, which led to the formation of down-faulted block under VES 3. The study area could be subdivided into two zones differing in their resistivities and depths. This study also proved that, the deepest subsided block, which involves VES 3, occupies the central part of the study area. These geoelectric interpretation results were confirmed by the drilled wells data of the drillhole No.3, at which VES 3 site was chosen.

Drilled well results were found throughout the study area and near to the locations of VESes, supported the results of seismic refraction and resistivity sounding. The depth to the surface of groundwater increased towards the northeastern and southwestern parts of the study area. Meanwhile, it decreased towards the northwestern and central parts. The very low radioactivity measured in the logs indicated that the aquifer is clean from this point of view.

## References

1. **Abdellatif, T.A., Galal, G.H. and Yousef, A.M.A., 1997**, Structural and lithological impact on the ground water occurrences along Wadi El Naqra-Wadi Bedaa area. Proc 15th An. Meet., Egypt, Geoph. Soc (EGS), pp.107-124.
2. **Abuelata, A.S. and Hassanein, A.G., 1990**, Comparative study of the geoelectric characteristics and water qualities in the Cairo-Suez and Cairo-Sokhna roads, Eastern Desert, Egypt. Mansoura Sci. Bull., Fac. Sci., Mansoura University, Egypt V.17 No1, Supplement, pp.511-532.
3. **Abu-Elenain.F.M. and Ismaeil.A.S., 1995**, Petrography, geochemistry and depositional history of the Eocene rocks in the area between Northern Galala and Gabal Ataqa, Western Gulf of Suez, Egypt. Annals Geol.Suv.Egypt,

- Vol.XX ,pp.551-576.
4. **Bernard, J., 2003**, Short note on the principles of geophysical methods for groundwater investigations. [www.Terraplus.com](http://www.Terraplus.com) (info@terraplus.com).
  5. **Conoco, 1987**, Geological map of Egypt, Scale 1:500,000, NH36 SW-BENI SUEF sheet.
  6. **Elbehiry, M.G., Shideed, A.G. and Elhusseiny, M.S., 2004**, Geographic Information System and remote sensing application for water resources: Wadi Ghoweibba Basin, West Gulf of Suez, Egypt. 7th Internat. Conf. on Geol. Arab World, Cairo Univ, Egypt, p.22.
  7. **Eldiasty, M.I., Elhakeim, B.E.A. and Saber, H.S.M., 1981**, carried out some recent geophysical well logging investigations in mining and ground water prospect in Ain El-Sokhna, Abu Tartur and Maghara. which, different bore hole are drilled in the area to study the geological section and geophysical parameters.
  8. **Galfi J. and Palos M., 1970**, Bulletin of the Intern Assoc. of Scientific Hydrology, XV, pp. 41-48.
  9. **Griffiths, D. and Turnbull, J., 1985**, A multi-electrode array for resistivity surveying. First Break, 3, No. (7), .pp:16–20.
  10. **Reynolds, J. W., 1997**, An introduction to applied and environmental geophysics. New York, USA, 796p.
  11. **Sadek, H. S., Soliman, S. A. and Abdulhady, H. M., 1989**, Correlation between different models of resistivity sounding data to discover new fresh water fields in Elsadat City, Western Desert, Egypt. Proc. of the 7th International Mathematical Geophysics Seminar, Free University of Berlin, Western Germany 8-11 Feb., 1989, pp. 329-346.
  12. **Said, R., 1990**, The geology of Egypt. Rotterdam Pup.Co,722p.
  13. **Salem, A. S., 1988**, Geological and hydrogeological studies on the area between Gabal Ataqa and Northern Galala plateau, Egypt.Ph.D., Fac .Sci, Geol. Dept, Zagazig Univ, Egypt, 271p.
  14. **Velpen, B. P. A., 1988**, Resist program, V. 1.0. M.Sc Research project, ITC, Holland.
  15. **Winsism, V.11 2009**, <http://www.wgeosoft.h> Seismic refraction processing software.
  16. **Youssef, M. I. and Abdel Rahman, M. A., 1978**, Structural map sensing of the area between Gabal Ataqa and northern Galala plateau, Gulf of Suez region, Egypt.Tenth Arab petroleum conference, Trippoli, Libya, 135(C-3) 8p.
  17. **Zohdy, A. A. R., 1974**, Use of Dar Zarrouk curves in the interpretation of vertical electrical sounding data; U.S. Geol. Surv. Bull., 1313-D, 41 p.
  18. **Zohdy, A. A. R., and Bisdorf, R., 1989**, A program for automatic processing and interpretation of Schlumberger sounding curves in Quick Basic 4.0. U. S. Geological Survey, Open - File Report, 89-137, 67 p.

4/22/2013